Statistics and Its Interface Volume 16 (2023) 189–197

# Quantile recurrent forecasting in singular spectrum analysis for stock price monitoring

Atikur R. Khan and Hossein Hassani*

Monitoring of near real-time price movement is necessary for data-driven decision making in opening and closing positions for day traders and scalpers. This can be done effectively by constructing a movement path based on forecast distribution of stock prices. High frequency trading data are generally noisy, nonlinear and nonstationary in nature. We develop a quantile recurrent forecasting algorithm via the recurrent algorithm of singular spectrum analysis that can be implemented for any type of time series data. When applied to median forecasting of deterministic and short- and long-memory processes, our quantile recurrent forecast overlaps the true signal. By estimating only the signal dimension number of parameters, this method can construct a recurrent formula by including many lag periods. We apply this method to obtain median forecasts for Facebook, Microsoft, and SNAP's intraday and daily closing prices. Both for intraday and daily closing prices, the quantile recurrent forecasts produce lower mean absolute deviation from original prices compared to bootstrap median forecasts. We also demonstrate the tracing of price movement over forecast distribution that can be used to monitor stock prices for trading strategy development.

AMS 2000 subject classifications: Primary 37M10, 91B84; secondary 90B50.
Keywords and phrases: Forecast distribution, Recurrent forecasting, Quantile, Trading.

## 1. INTRODUCTION

Closing stock prices are of interest in trading strategy development. Accurately predicting a stock market is of great interest to many stakeholders to make a profit and guard their investments against risks. Stock price monitoring and forecasting play important role in trading strategy development and investment decision making [1, 2]. Stock prices are noisy and very often they are non-normal, nonstationary and nonlinear [3, 4, 5]. Generating signals from noisy price movement requires not only market monitoring skill but also requires to choose a flexible model that can adapt to changing pattern in the market. Singular spectrum analysis (SSA) is a nonparametric method that is deemed to be suitable for extracting and forecasting signals from linear, nonlinear, stationary, and nonstationary time series [6]. For recent application of SSA techniques in finance and economics see for example [7, 8, 9, 10]. We apply this method to develop future paths of stock prices and use these paths to trace price movement to enable trading decision making.

With the advancement of machine learning in financial time series analysis, artificial neural network (ANN), random forest (RF) and support vector regression (SVR) gain popularity in predicting stock prices [11, 12, 13, 14]. Hybrid modelling approaches have also been widely implemented in forecasting stock prices [15, 5, 16]. Ticknor [13] implemented Bayesian regularized artificial neural network (BRANN) for one day ahead forecasting of closing prices in response to several technical indicators. Lu and Wu [1] used neural networks and SVR for forecasting daily Nikkei 225 and TAIEX closing cash indexes. In an attempt to forecast daily closing stock prices, Pai and Lin [15] have fitted an autoregressive integrated moving average (ARIMA) model to obtain forecast and then SVR forecast of the residual series is added to the ARIMA forecast. Their hybrid model has been evaluated by computing one-step ahead forecast error. Hybrid models are subjective in nature and a single approach may not be suitable for varied data types.

Stock prices are noisy in nature and hybrid modelling approaches in [5], [17], and [14] considered noise reduction approaches as a preprocessing step to model building and forecasting. The ICA-BPN prediction model [5] utilizes independent component analysis (ICA) to filter out the noise contained in forecasting variables and then uses these variables in back-propagation neural network (BPN) for construction of a forecasting model. Kao et al. [14] have applied wavelet transformation for feature extraction and passed these features to a SVR model to forecast stock prices. Akin to the works in [5] and [14], SSA can be used to extract features from historical time series of stock prices and these features can be used further to obtain forecasts.

Forecasting a daily closing price is commonly adopted approach in decision making and can be done by implementing any of these predictive models. But a vision for subsequent price distribution is more appealing to investors for trading strategy development. An investor or a day trader is more likely to view price distribution for several subsequent days for trading strategy development. Whereas a scalper may wish to view probable price paths for subsequent time points for intraday trading. This can effectively

*Corresponding author.

be done by forecasting quantiles of closing prices and constructing price paths for future time points. Hagfors et al. [18] have explored electricity price distribution by estimating coefficients for different quantiles in quantile regression. Nowotarski and Weron [19] constructed prediction intervals by averaging ensemble of point forecasts from quantile regression of electricity spot prices. Thus we may apply SSA to filter out noise to extract features and then use these features to construct ensemble of forecasts from quantile regression. This will provide a distribution of prices for subsequent future time points. To construct ensemble of forecasts for quantiles via SSA, we develop a quantile recurrent forecasting method in SSA.

To organize rest of the paper we provide a detailed exposition of SSA methods for forecasting and develop quantile recurrent forecasting method in Section 2. In Section 3, we provide simulation results for quantile recurrent forecasting for deterministic cosinusoidal and short-and long-memory processes. We apply this method to obtain quantile forecasts for daily and intraday closing stock prices of Facebook, Microsoft and SNAP. The selection of Facebook, Microsoft, and SNAP is just for the applicability of the proposed approach, while the proposed algorithm can be utilized for other social media and data providers. We also demonstrate the continuous monitoring of stock prices over price paths of quantile forecasts in Section 4 and provide concluding remarks in Section 5.

## 2. SSA FORECASTING

There are two different algorithms in forecasting via SSA namely the recurrent forecasting and vector forecasting. Both of these forecasting algorithms require to follow two common steps of SSA, the decomposition and reconstruction of a time series. In this section, we provide a brief description of forecasting processes in SSA.

### 2.1 Decomposition and reconstruction of time series

In SSA, we embed the time series $\{x_1, x_2, \ldots, x_N\}$ into a high-dimensional space by constructing a Hankel structured trajectory matrix of the form

$$(1) \qquad \boldsymbol{X} = \begin{pmatrix} x_1 & x_2 & x_3 & \ldots & x_n \\ x_2 & x_3 & x_4 & \ldots & x_{n+1} \\ \vdots & \vdots & \vdots & \ldots & \vdots \\ x_m & x_{m+1} & x_{m+2} & \ldots & x_N \end{pmatrix} = [\boldsymbol{x}_1 \quad \ldots \quad \boldsymbol{x}_i \quad \ldots \quad \boldsymbol{x}_n],$$

where $m$ is the window length, the $m$-lagged vector $\boldsymbol{x}_i = (x_i, x_{i+1}, \ldots, x_{i+m-1})'$ is the $i$th column of the trajectory matrix $\boldsymbol{X}$, $n = N - m + 1$ and $m \leq n$.

The singular value decomposition (SVD) of the trajectory matrix $\boldsymbol{X}$ can be expressed as

$$(2) \qquad \boldsymbol{X} = \boldsymbol{S}_k + \boldsymbol{E}_k = \sum_{j=1}^{k} \sqrt{\lambda_j}\boldsymbol{u}_j\boldsymbol{v}_j' + \sum_{j=k+1}^{m} \sqrt{\lambda_j}\boldsymbol{u}_j\boldsymbol{v}_j'$$

where $\boldsymbol{u}_j$ is the $j$th eigenvector of $\boldsymbol{X}\boldsymbol{X}'$ corresponding to the eigenvalue $\lambda_j$ and $\boldsymbol{v}_j = \boldsymbol{X}'\boldsymbol{u}_j/\sqrt{\lambda_j}$.

If $k$ is the number of signal components, $\boldsymbol{S}_k = \sum_{j=1}^{k} \sqrt{\lambda_j}\boldsymbol{u}_j\boldsymbol{v}_j'$ represents a matrix of signal and $\boldsymbol{E}_k = \sum_{j=k+1}^{m} \sqrt{\lambda_j}\boldsymbol{u}_j\boldsymbol{v}_j'$ is the matrix of noise. We apply diagonal averaging procedure to $\boldsymbol{S}_k$ to reconstruct signal series $\widetilde{s}_t$ such that the observed series can be expressed as

$$(3) \qquad x_t = \widetilde{s}_t + \widetilde{e}_t,$$

where $\widetilde{e}_t$ is the filtered out noise series. A detailed exposition of decomposition in Eq. (3) can be found in Khan and Poskitt [20].

It is worth mentioning that the selection of the SSA parameters/choices depends on various factors, but the general concept is to achieve minimal errors. As illustrated above, we deal with a basic time series model, 'signal + noise.' Thus, the residual pattern after signal extraction informs us if the selected parameters are appropriately done.

### 2.2 Recurrent forecast

The reconstructed signal matrix derived from the first $k$ signal components can be written as

$$(4) \qquad \boldsymbol{S}_k = \sum_{i=1}^{k} \boldsymbol{X}_i = \sum_{i=1}^{k} \boldsymbol{u}_i\boldsymbol{u}_i'\boldsymbol{X} = \boldsymbol{U}_k\boldsymbol{U}_k'\boldsymbol{X},$$

where $m \times k$ matrix $\boldsymbol{U}_k = [\boldsymbol{u}_1 : \ldots : \boldsymbol{u}_k]$ is the matrix of $k$ eigenvectors of $\boldsymbol{X}\boldsymbol{X}'$. Now we partition the matrix $\boldsymbol{U}_k$ such that $\boldsymbol{U}_k = \left(\boldsymbol{U}_k'^{\,u}\ \boldsymbol{U}_k'^{\,l}\right)'$ where $\boldsymbol{U}_k^l$ is the row vector of elements in the last row of $\boldsymbol{U}_k$ and $\boldsymbol{U}_k^u$ is a $(m-1) \times k$ matrix of the first $m-1$ rows of $\boldsymbol{U}_k$. Partitioning $\boldsymbol{S}_k$ and $\boldsymbol{X}_k$ conformable with the partition of $\boldsymbol{U}_k$ in Eq. (4) can be rewritten as

$$(5) \qquad \begin{pmatrix} \boldsymbol{S}_k^u \\ \boldsymbol{S}_k^l \end{pmatrix} = \begin{pmatrix} \boldsymbol{U}_k^u \\ \boldsymbol{U}_k^l \end{pmatrix} \begin{pmatrix} \boldsymbol{U}_k^{u'} & \boldsymbol{U}_k^{l'} \end{pmatrix} \begin{pmatrix} \boldsymbol{X}^u \\ \boldsymbol{X}^l \end{pmatrix} = \begin{pmatrix} \boldsymbol{U}_k^u\boldsymbol{U}_k^{u'}\boldsymbol{X}^u + \boldsymbol{U}_k^u\boldsymbol{U}_k^{l'}\boldsymbol{X}^l \\ \boldsymbol{U}_k^l\boldsymbol{U}_k^{u'}\boldsymbol{X}^u + \boldsymbol{U}_k^l\boldsymbol{U}_k^{l'}\boldsymbol{X}^l \end{pmatrix}.$$

The projection of the last row of signal matrix $\boldsymbol{S}_k$ on to its first $m-1$ rows is defined by

(6)
$$\begin{aligned}
\boldsymbol{S}_k^l &= \boldsymbol{U}_k^l \boldsymbol{U}_k^{u'} \boldsymbol{X}^u + \boldsymbol{U}_k^l \boldsymbol{U}_k^{l'} \boldsymbol{X}^l \\
&= \boldsymbol{U}_k^l \boldsymbol{U}_k^{u'} (\boldsymbol{S}_k^u + \boldsymbol{E}_k^u) + \boldsymbol{U}_k^l \boldsymbol{U}_k^{l'} (\boldsymbol{S}_k^l + \boldsymbol{E}_k^l) \\
&= (1 - \boldsymbol{U}_k^l \boldsymbol{U}_k^{l'})^{-1} [\boldsymbol{U}_k^l \boldsymbol{U}_k^{u'} (\boldsymbol{S}_k^u + \boldsymbol{E}_k^u) + \boldsymbol{U}_k^l \boldsymbol{U}_k^{l'} \boldsymbol{E}_k^l] \\
&= (1 - \boldsymbol{U}_k^l \boldsymbol{U}_k^{l'})^{-1} \boldsymbol{U}_k^l \boldsymbol{U}_k^{u'} \boldsymbol{S}_k^u \\
&\qquad + (1 - \boldsymbol{U}_k^l \boldsymbol{U}_k^{l'})^{-1} \boldsymbol{U}_k^l [\boldsymbol{U}_k^{u'} \boldsymbol{E}_k^u + \boldsymbol{U}_k^{l'} \boldsymbol{E}_k^l] \\
&= (1 - \boldsymbol{U}_k^l \boldsymbol{U}_k^{l'})^{-1} \boldsymbol{U}_k^l \boldsymbol{U}_k^{u'} \boldsymbol{S}_k^u + (1 - \boldsymbol{U}_k^l \boldsymbol{U}_k^{l'})^{-1} \boldsymbol{U}_k^l \boldsymbol{U}_k' \boldsymbol{E}_k \\
&= (1 - \boldsymbol{U}_k^l \boldsymbol{U}_k^{l'})^{-1} \boldsymbol{U}_k^l \boldsymbol{U}_k^{u'} \boldsymbol{S}_k^u \\
&\qquad + (1 - \boldsymbol{U}_k^l \boldsymbol{U}_k^{l'})^{-1} \boldsymbol{U}_k^l [\boldsymbol{U}_k' \boldsymbol{U}_{m-k} \boldsymbol{U}_{m-k}' \boldsymbol{X}] \\
&= (1 - \boldsymbol{U}_k^l \boldsymbol{U}_k^{l'})^{-1} \boldsymbol{U}_k^l \boldsymbol{U}_k^{u'} \boldsymbol{S}_k^u,
\end{aligned}$$

where $\boldsymbol{a}' = (1 - \boldsymbol{U}_k^l \boldsymbol{U}_k^{l'})^{-1} \boldsymbol{U}_k^l \boldsymbol{U}_k^{u'}$ is the vector of coefficients for the projection of $\boldsymbol{S}_k^l$ on $\boldsymbol{S}_k^u$ and is used to construct a linear recurrent formula.

Recurrent forecasting in SSA is also known as *R-forecasting* and is the most popular forecasting algorithm in SSA [21]. If $\boldsymbol{u}_j^u = (u_{1j}, \ldots, u_{(m-1)j})'$ is the vector of the first $m-1$ elements of the $j$th eigenvector $\boldsymbol{u}_j$ and $u_{mj}$ is the last element of $\boldsymbol{u}_j$, coefficients of linear recurrent equation can be estimated as

$$\boldsymbol{a} = (a_{(m-1)}, \ldots, a_1)' = \frac{1}{1 - \sum_{j=1}^k u_{mj}^2} \sum_{j=1}^k u_{mj} \boldsymbol{u}_j^u. \tag{7}$$

With the parameters in Eq. (7), a linear recurrent equation of the form

$$\widetilde{s}_t = \sum_{i=1}^{m-1} a_{(m-i)} \widetilde{s}_{t-m+i} \tag{8}$$

is used to obtain one-step ahead recursive forecast [20, 22, 6]. This linear recurrent formula in Eq. (8) is used to forecast the signal at time $t+1$ given the signal at time $t, t-1, \ldots, t-m+2$ [21, sec. 2.1, eq. 2.1-2.2] and the one-step-ahead recursive forecast of $x_{N+j}$ is

(9)
$$\hat{s}_{N+j} = \begin{cases} \sum_{i=1}^{j-1} a_i \hat{s}_{N+j-i} + \sum_{i=1}^{m-j} a_{m-i} \widetilde{s}_{N+j-m+i} \\ \qquad \text{for } j \le m-1; \\ \sum_{i=1}^{m-1} a_i \hat{s}_{N+j-i} \text{ for } j > m-1. \end{cases}$$

### 2.3 Quantile recurrent forecast

As can be seen in Eq. (6), the last row of the reconstructed trajectory matrix is

$$\boldsymbol{S}_k^l = (1 - \boldsymbol{U}_k^l \boldsymbol{U}_k^{l'})^{-1} \boldsymbol{U}_k^l \boldsymbol{U}_k^{u'} \boldsymbol{S}_k^u,$$

and by adding the noise part $\boldsymbol{E}_k^l$ on both sides we may write that

$$\begin{aligned}
\boldsymbol{X}^l &= (1 - \boldsymbol{U}_k^l \boldsymbol{U}_k^{l'})^{-1} \boldsymbol{U}_k^l \boldsymbol{U}_k^{u'} \boldsymbol{S}_k^u + \boldsymbol{E}_k^l \\
&= (1 - \boldsymbol{U}_k^l \boldsymbol{U}_k^{l'})^{-1} \boldsymbol{U}_k^l \left( \boldsymbol{U}_k^{u'} \boldsymbol{S}_k^u \right) + \boldsymbol{E}_k^l \\
&= \boldsymbol{\beta} \left( \boldsymbol{U}_k^{u'} \boldsymbol{S}_k^u \right) + \boldsymbol{E}_k^l. \qquad (10)
\end{aligned}$$

Applying a transpose to the above equation, Eq. (10), we can write

$$\begin{aligned}
(\boldsymbol{X}^l)' &= \left( \boldsymbol{U}_k^{u'} \boldsymbol{S}_k^u \right)' \boldsymbol{\beta}' + (\boldsymbol{E}_k^l)' \\
&\Rightarrow \boldsymbol{y}^* = \boldsymbol{X}^* \boldsymbol{\alpha} + \boldsymbol{\epsilon} \qquad (11)
\end{aligned}$$

where $\boldsymbol{\alpha} = \boldsymbol{\beta}'$ is a vector of $k$ parameters, $\boldsymbol{X}^* = \left( \boldsymbol{U}_k^{u'} \boldsymbol{S}_k^u \right)'$, $\boldsymbol{\epsilon} = \left( \boldsymbol{E}_k^l \right)'$, and $\boldsymbol{y}^*$ is the last row of the trajectory matrix $\boldsymbol{X}$.

In SSA, we estimate coefficients of the linear recurrent equation and there are $m-1$ number of parameters that are estimated naturally from the decomposition of the trajectory matrix $\boldsymbol{X}$. But Eq. (11) has only $k$ parameters that can regulate the distribution of $m-1$ parameters under the transformation. If $\boldsymbol{\alpha}$ is estimated as in quantile regression to obtain median forecast, this can be transferred back to form a quantile recurrence formula with $m-1$ coefficients. This procedure is suitable at least when an analyst requires to consider too many time lags for quantile forecasting. We only need to estimate $k$ number of parameters to unveil a quantile recurrence formula with $m-1$ parameters even when $m$ is much higher than $k$.

The quantile regression estimate of $\boldsymbol{\alpha}$ can be obtained by solving the equation

$$\hat{\boldsymbol{\alpha}} = argmin_{\boldsymbol{\alpha}} \sum \rho_\tau \left( y_i^* - \boldsymbol{x}_i^{*'} \boldsymbol{\alpha} \right) \tag{12}$$

where $0 < \tau < 1$ represents the probability and

$$\rho_\tau(z) = \begin{cases} z(\tau - 1) & \text{for } z < 0; \\ z\tau & \text{for } z \ge 0. \end{cases}$$

Setting $\tau = 0.5$ will provide estimates for $\boldsymbol{\alpha}$ leading to the median regression. Thus $\hat{\boldsymbol{\beta}}_\tau = \hat{\boldsymbol{\alpha}}'$ and the quantile recurrence relationship can be written as

$$\boldsymbol{S}_k^l = \hat{\boldsymbol{\beta}}_\tau \boldsymbol{U}_k^{u'} \boldsymbol{S}_k^u = \hat{\boldsymbol{\beta}}_\tau^* \boldsymbol{S}_k^u \tag{13}$$

where $\hat{\boldsymbol{\beta}}_\tau^* = \hat{\boldsymbol{\beta}}_\tau \boldsymbol{U}_k^{u'}$ is a $m-1$ vector of quantile recurrent coefficients, and the recurrence relationship

$$\widetilde{s}_{k,\tau}(t) = \sum_{j=1}^{m-1} \hat{\beta}_{\tau,j}^* \widetilde{s}_k(t-m+j) \tag{14}$$

provides one-step ahead recursive quantile forecast.

## 3. NUMERICAL ILLUSTRATION

### 3.1 Deterministic cosinusoidal process

Sinusoidal signals are commonly used in engineering and physics. Many literatures on SSA also used the examples of cosine and exponentially modulated series [21, 23, 24, 25]. Here we consider an example of cosine series generated as

$$y_t \quad = \quad \mu + \sum_{r=1}^{p} A_r cos(\lambda_r t + \theta_r) + \epsilon_t$$

where $\mu$ is the mean signal, $A_r$ is the amplitude, $\lambda_r$ is the frequency (number of cycles per unit measured in radians), $\theta_r$ is the phase uniformly distributed over the range $(-\pi, \pi)$ and $\epsilon_t$ is the i.i.d. Gaussian noise process with noise variance $\sigma^2$. The wavelength of the process is $2\pi/\lambda_r$. This series has previously been used in [26].

Since the amplitude $A_r$ and the frequency $\lambda_r$ are constant at time $t$, we may write

$$E(y_t y_{t+h}) = \begin{cases} \mu^2 + \frac{1}{2}\sum_{r=1}^{p} A_r^2 cos(\lambda_r h) & \text{if } h \neq 0; \\ \mu^2 + \frac{1}{2}\sum_{r=1}^{p} A_r^2 + \sigma^2 & \text{if } h = 0. \end{cases}$$

Therefore, $\{y_t\}$ is deemed to be a stationary process and possess a linear recurrent formula (LRF) of dimension $2p+1$. Signal-to-noise ratio (SNR) of this process is

$$SNR = 10\log_{10}\left(\frac{\mu^2 + \frac{1}{2}\sum_{r=1}^{p} A_r^2}{\sigma^2}\right) \text{ dB.}$$

By setting different values to this signal-to-noise ratio, we may generate data for further analysis. For instance, let us consider the following setup for a data generating process (DGP)

(15)

$$y_t = 0.75 + 3cos(2\pi t/7 + \pi/5) + 1.5cos(2\pi t/10 - \pi/4) + \epsilon_t$$

where a Gaussian noise process is added such that noise variance satisfies certain level of signal-to-noise ratio. In practice, we generate data for different noise variance $\sigma^2$ by controlling the SNR level such that $SNR = 10log_{10}\left(\frac{6.1875}{\sigma^2}\right)$ decibel (dB).

We generate 1,000 time series of length $N = 200$ form Eq. (15) by setting $SNR = 10\ dB$ and obtain $h = 12$ forecasts from each of the generated series by using recurrent forecasting algorithm of $SSA(100, k)$ model (SSA with window length $\lfloor N/2 \rfloor$ and number of component $k$ selected by employing the description length criterion) and plot the median and quartiles of forecasts in Figure 1. We also compute quantile forecast via SSA (QSSA) and plot medians of quartile forecasts in Figure 1. Both the median forecasts from QSSA and SSA overlap the true signal, and the quartile forecasts are hardly distinguishable. Thus it mimics that the QSSA forecast is providing qualitatively similar distributional properties of SSA forecast. Similar results are obtained when data is generated by setting $SNR = 5\ dB$, as can be seen in Figure 2.

## 3.2 Short-and long-memory processes

Assuming $\epsilon_t$ being a white noise process, let us define an $AR(2)$ process of the form

$$(1 - 0.8B)(1 - 0.6B)x_t = \epsilon_t. \tag{16}$$

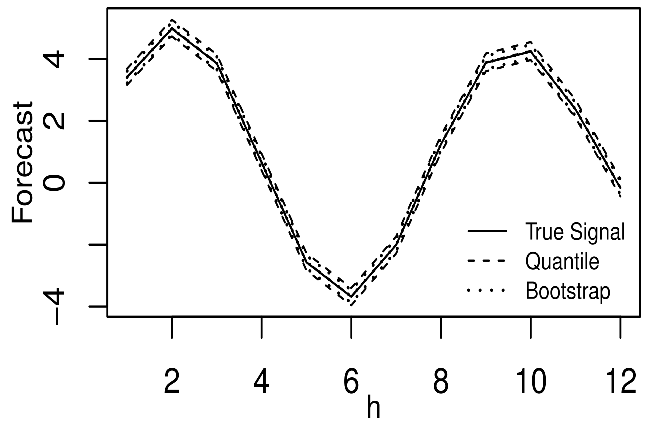


*Figure 1. Median and quartile forecasts obtained from bootstrapping and quantile SSA of cosinusoidal signal when* $SNR = 10\ dB$.

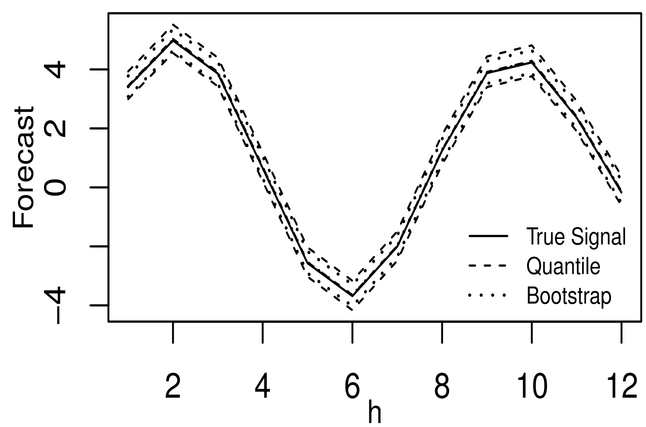


*Figure 2. Median and quartile forecasts obtained from bootstrapping and quantile SSA of cosinusoidal signal when* $SNR = 5\ dB$.

This $AR(2)$ process has previously been studied explicitly in [27, Example 25.1, p.57] for an autoregressive process with real roots within the unit circle.

Assuming Gaussian white noise process, we generate 1,000 time series of length $N = 200$ from the $AR(2)$ process in Eq. (16) and for each of the series we obtain $h = 12$ forecasts from $SSA(100, k)$ models as has been described in Section 3.1. Quartiles of forecasts obtained from $SSA(100, k)$ models are displayed in Figure 3. We also compute medians of quantile forecasts for each of the quartiles from QSSA forecast. Akin to the results in Figure 1 and Figure 2, the median forecast from both methods are hardly distinguishable from the true signal ($E(x_t) = 0$) and the quartile forecasts are lying very close to each other. Thus both SSA and QSSA provide qualitatively similar forecast distribution for this short-memory process.

To introduce long-memory in Eq. (16) we consider a fractional differencing parameter $d = 0.3$ and define a process

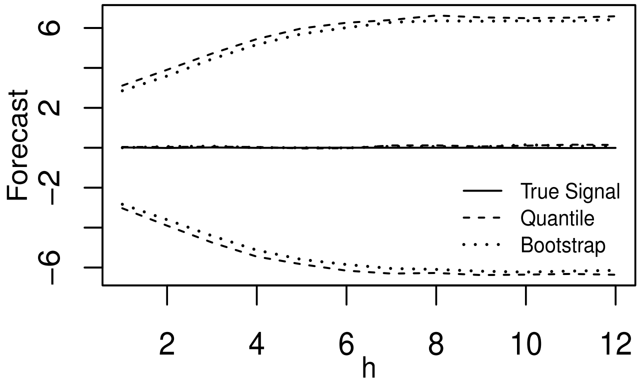


*Figure 3. Median and quartile forecasts obtained from bootstrapping and quantile SSA of $AR(2)$ process in Eq (16).*

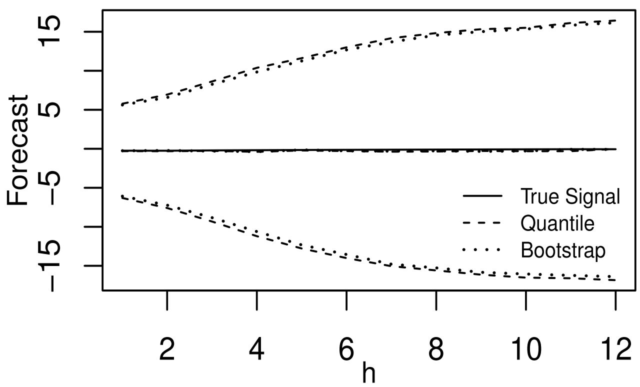


*Figure 4. Median and quartile forecasts obtained from bootstrapping and quantile SSA of $FAR(2)$ process in Eq (17).*

of the form

$$(1 - 0.8B)(1 - 0.6B)(1 - B)^{0.3}x_t = \epsilon_t \tag{17}$$

where $\epsilon_t \sim WN(0, 1)$. We generate 1,000 time series of length $N = 200$ and obtain forecasts both from SSA and QSSA by following the procedures described above for the short-memory process. Forecast quantiles are provided in Figure 4. We find that both forecasting algorithms provide qualitatively similar results with median forecasts lying on the true signal. Results obtained from both simulation experiments demonstrate that the quantile forecasting methods in SSA performs qualitatively similar to the recurrent forecasting method.

## 4. PRACTICAL APPLICATION

We have demonstrated through simulation experiments that the utilization of QSSA may produce quantile forecasts qualitatively very similar to the bootstrap quantiles of SSA. In this section, we apply quantile SSA and bootstrap SSA methods to obtain median forecast of intraday and daily closing prices of major social media stocks.

### 4.1 Intraday closing prices

We obtain intraday minute level closing prices data of Facebook (FB), Microsoft (MSFT) and SNAP from "2019-10-31 12:01:00" to "2019-11-01 12:30:00". For each of the ticker time series, we leave the last 30 minutes data for testing and use the remaining data as training data for model fitting. Tickers data shown in Figure 5 are extracted by implementing the `R` package `quantmod`.

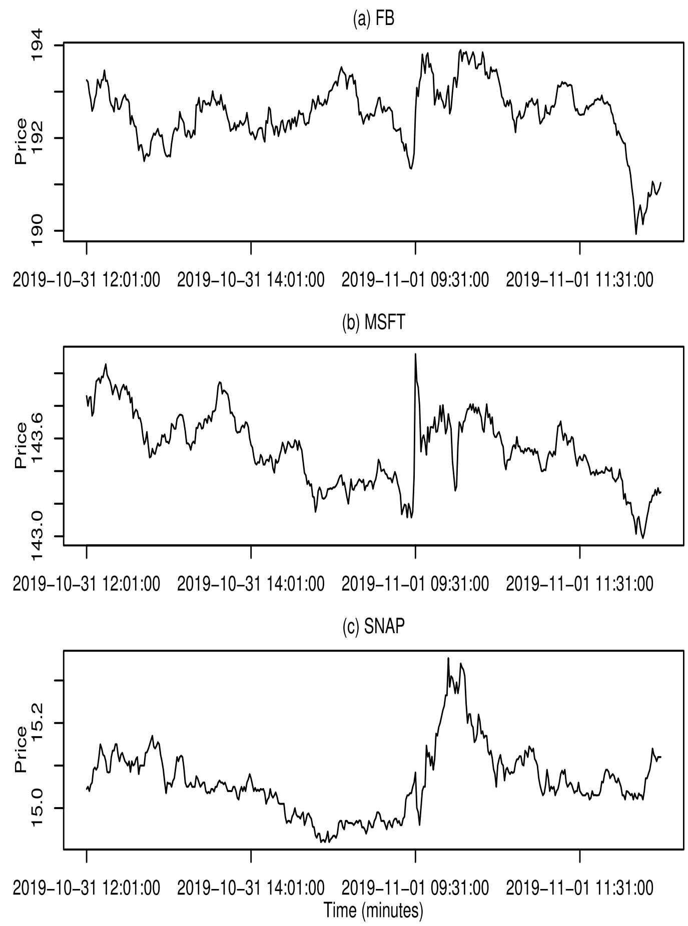


*Figure 5. Intraday closing prices of (a) Facebook (FB) (b) Microsoft (MSFT) and (c) SNAP from "2019-10-31 12:01:00" to "2019-11-01 12:30:00".*

We apply Jarque-Bera test [28, 29] for normality, Kwiatkowski-Phillips-Schmidt-Shin (KPSS) test [30] for stationarity and Teraesvirta NN test [31] for linearity to these data sets, and provide these test results in Table 1. Though the KPSS test rejects the stationarity of these data sets, the TNN test supports the linearity. The normality of FB closing price is supported by the Jarque-Bera test, but the normality is rejected for MSFT and SNAP intraday closing prices. SSA can be applied to non-normal and nonstationary

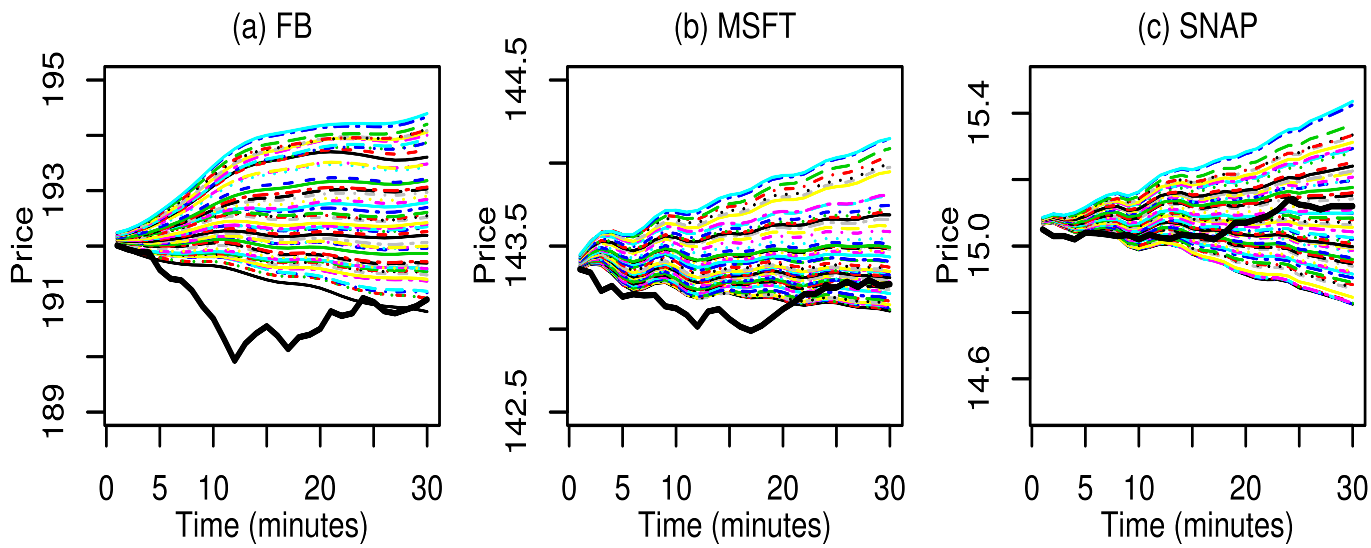


*Figure 6. Forecast distribution of intraday (minutes) closing prices of (a) Facebook (FB) (b) Microsoft (MSFT) (c) SNAP, where the thick solid line is the original price and colored lines are 20% to 80% quantile forecasts.*

time series without any transformation, and we apply SSA to analyze these data sets.

*Table 1. Statistical properties of daily closing prices of tickers FB, MSFT, and SNAP*

| | Jarque-Bera Test | | KPSS Test | | TNN Test | |
|---|---|---|---|---|---|---|
| Ticker | $\chi^2$ | Normal | $KPSS$ | STS | $\chi^2$ | Linear |
| FB | 1.70 | Yes | 1.23 | No | 0.09 | Yes |
| MSFT | 7.01 | No | 1.59 | No | 0.06 | Yes |
| SNAP | 61.95 | No | 0.71 | No | 2.17 | Yes |

Here, STS refers to stationarity of time series.

We select an hour window (window length $m = 60$) for construction of trajectory matrix and apply the $SDL(k|m)$ criterion of Khan and Poskitt [32] to select the number of signal components for SSA of historical training data. Median forecasts are obtained both from bootstrapping of SSA and quantile recurrent forecasting. Mean absolute deviation (MAD) of forecast from observed prices are computed by using the following formula

$$MAD(h) = \frac{1}{h}\sum_{j=1}^{h} |x_{N+j} - \hat{x}_{N+j}|$$

where $\hat{x}_{N+j}$ is the median forecast corresponding to $x_{N+j}$.

Results in Table 2 reveal that the median forecast from quantile SSA provides lower MAD compared to bootstrap median of minute level closing prices. For FB closing prices, QSSA provides around 10% less MAD than that of bootstrap median forecast in SSA. We find that both for 15 minutes and 30 minutes ahead recursive median forecasting QSSA provides relatively better results than the bootstrap median forecast from SSA.

*Table 2. Mean absolute deviation of median forecast of a minute closing prices of social media tickers*

| | $h = 15$ | | | $h = 30$ | | |
|---|---|---|---|---|---|---|
| Ticker | QSSA | BSSA | $\frac{QSSA}{BSSA}$ | QSSA | BSSA | $\frac{QSSA}{BSSA}$ |
| FB | 1.20 | 1.32 | 0.91 | 1.44 | 1.60 | 0.90 |
| MSFT | 0.20 | 0.23 | 0.87 | 0.19 | 0.23 | 0.83 |
| SNAP | 0.04 | 0.06 | 0.67 | 0.04 | 0.05 | 0.80 |

Here, $\frac{QSSA}{BSSA}$ is the relative $MAD(h)$ of QSSA with respect to BSSA.

Though the median forecasts are useful to learn about the future closing prices of a stock, it is of interest to stock marketing analysts that the future closing prices can be tracked over the forecast distribution. In stock prices, analysts are more interested in prices between the first and the third quartiles. Thus we compute 20% to 80% quantile forecasts of minutes closing prices and plot these forecasts in Figure 6.

Forecast distribution of FB clearly shows that the closing minute prices are moving further down from the 20% quantile forecast and is not likely to return to the median level in the next subsequent minutes. After 15 minutes price starts to rise but clearly it is highly unlikely to cross the lower quartile forecast. This movement tracing will help an analyst to make a quick trading decision.

Minute closing price of MSFT is moving down of the 20% quantile forecast and its seems that even after 15 minutes the price is less likely to return to its median forecast. By comparing the movement of original price with respect to the forecast distribution, it can be assumed by an analyst that the future closing prices are not moving up to and above the median forecast in the next subsequent minutes. Unlike the closing prices of FB and MSFT, minute closing price of

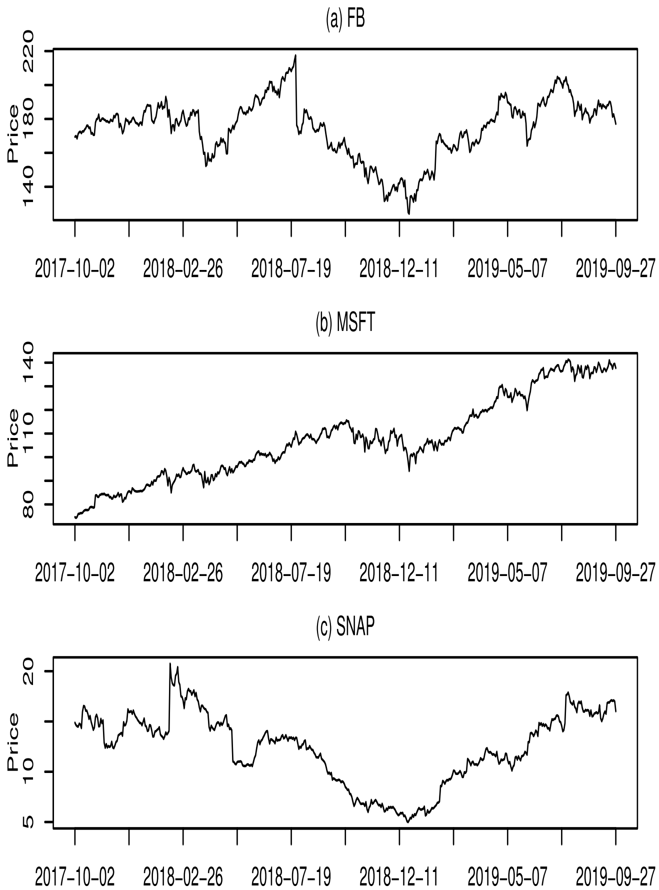


*Figure 7. Daily closing prices of (a) Facebook (FB) (b) Microsoft (MSFT) and (c) SNAP from "2017-10-01" to "2019-09-30".*

SNAP starts moving around the first quartile of the forecast distribution and around 15 minutes later the price swings up and indicates a trend to return to the median forecast. Tracing of price movement on the forecast distribution can help a trading analyst to trace its position after the next subsequent minutes to build a trading strategy.

## 4.2 Daily closing prices

We obtain 'daily closing prices data of Facebook (FB), Microsoft (MSFT) and SNAP from "2017-10-01" to "2019-09-30". For each of the ticker time series, we leave the last 10 business days (2 weeks) data for testing and use the remaining data as training data for model fitting. The `R` package `quantmod` has been used to extract these data sets from Yahoo Finance and are presented in Figure 7.

To explore statistical properties of these time series, we apply Jarque-Bera test [28, 29] for normality, Kwiatkowski-Phillips-Schmidt-Shin (KPSS) test [30] for stationarity and Teraesvirta NN test [31] for linearity to these data sets. Test results provided in Table 3 support that the daily FB and SNAP closing prices are non-normal, nonstationary and nonlinear. Daily closing price of MSFT is non-normal and nonstationary, but linearity is supported by the TNN test.

*Table 3. Statistical properties of daily closing prices of tickers FB, MSFT and SNAP*

| | Jarque-Bera Test | | KPSS Test | | TNN Test | |
|---|---|---|---|---|---|---|
| Ticker | $\chi^2$ | Normal | $KPSS$ | STS | $\chi^2$ | Linear |
| FB | 19.89 | No | 0.87 | No | 17.76 | No |
| MSFT | 19.557 | No | 7.29 | No | 1.94 | Yes |
| SNAP | 18.43 | No | 2.11 | No | 10.85 | No |

Here, STS refers to stationarity of time series.

It is known that SSA is suitable for time series of varied properties and can be used without any transformation even if the time series in non-normal, nonstationary and nonlinear in nature. We obtain median forecast from quantile SSA and bootstrap SSA and incorporate relative MAD values for 1 week (5 days) and 2 weeks (10 days) recursive forecasts. When compared to 5 days forecasting performance, the quantile SSA forecast provides much lower MAD than that of bootstrap median forecast. This property also reflects in 10 days recursive forecasting of closing prices. Thus for 5 days and 10 days recursive median forecasting, quantile recurrent forecasting provides better performance compared to bootstrap median forecast of SSA. Since the quantiles are distributed around the median, we apply recurrent quantile forecasting to trace movement of closing prices.

*Table 4. Mean absolute deviation of median forecast of daily closing prices of social media tickers*

| | $h = 5$ | | | $h = 10$ | | |
|---|---|---|---|---|---|---|
| Ticker | QSSA | BSSA | $\frac{QSSA}{BSSA}$ | QSSA | BSSA | $\frac{QSSA}{BSSA}$ |
| FB | 3.81 | 6.00 | 0.64 | 5.57 | 7.52 | 0.74 |
| MSFT | 3.51 | 5.02 | 0.70 | 6.44 | 8.07 | 0.80 |
| SNAP | 1.94 | 2.1 | 0.92 | 2.67 | 2.74 | 0.97 |

Here, $\frac{QSSA}{BSSA}$ is the relative $MAD(h)$ of QSSA with respect to BSSA.

By following the movement of FB closing prices over the forecast distribution in Figure 8, we explore that the closing price starts growing over the median forecast providing a signal that the price is likely to exceed the 80% quantile forecast in the next subsequent days. As soon as the price becomes stable over the 80% quantile position, it may swing upward further or may swing downward. We find that the price swings down towards the median and is likely to down further with a falling signal in closing price. The falling pattern clearly demonstrates that the price is likely to fall below the 20% quantile position in the next subsequent days.

The closing price of MSFT starts growing over the median and it provides a clear indication that the price is likely to cross the upper quartile forecast. Tracing the price movement over the forecast distribution clearly demonstrates that the price is trending over the 80% quantile position and

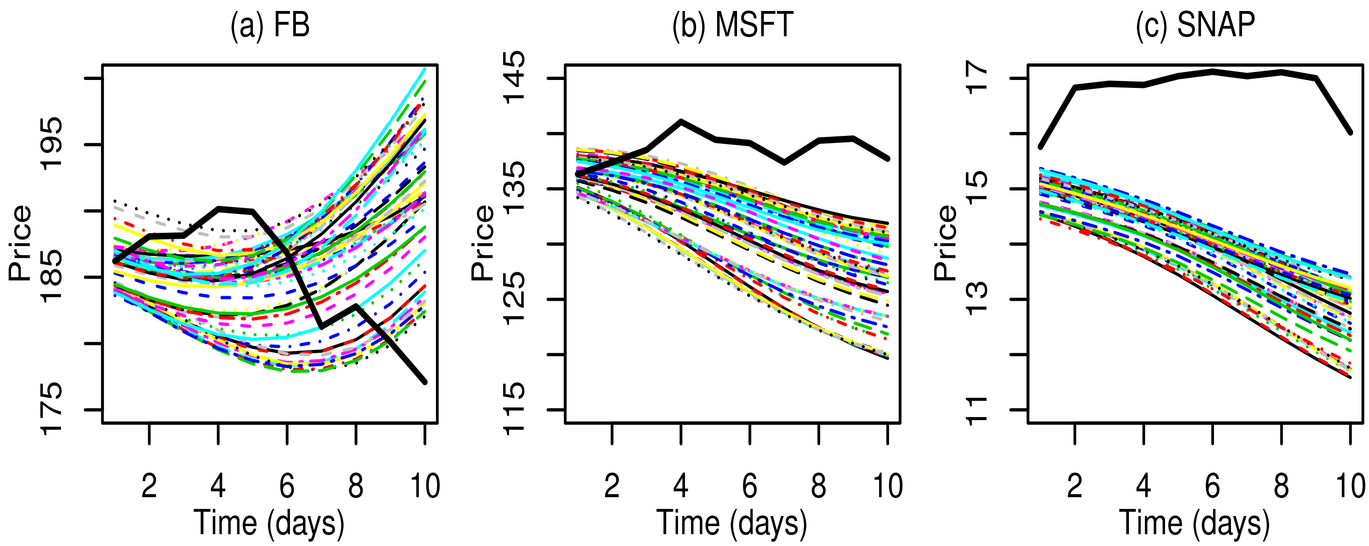


*Figure 8. Forecast distribution of daily closing prices of (a) Facebook (FB) (b) Microsoft (MSFT) and (c) SNAP, where the thick solid line is the original price and colored lines are 20% to 80% quantile forecasts.*

is less likely to fall below the third quartile of the forecast distribution. This signal can be used by a trading analyst to adopt a trading plan. Similarly, the SNAP closing price starts moving much over the 80% quantile of the forecast distribution and signals that the price is highly unlikely to cross below the third quartile of the distribution in the next subsequent days.

It seems that both for intraday and daily closing prices quantile recurrent forecasting provides much better results compared to bootstrap median forecast. Quantile recurrent forecasting also provides enough information about forecast distribution to monitor price movement for making trading decisions.

## 5. CONCLUDING REMARKS

Forecasting closing stock prices is a quintessential part in trading strategy development and decision making. A trading analyst may obtain forecasts by employing different statistical methods to enable data-driven decision making. Since the stock market is highly noisy and volatile, it is very important to monitor stock prices continuously to assess an adopted trading strategy. We develop a hybrid forecasting model by employing SSA to construct features and then use these features to construct ensemble of quantile forecasts. These ensemble of quantile forecasts can be used to construct a price distribution for future time points and stock prices can be monitored continuously by plotting available current prices on the constructed price distribution. This enables traders to follow-up stock prices on the price distribution for data-driven decision making. The study can be further enhanced by adding automated change point detection for various h-step ahead and its multivariate version. The issue of SSA parameters choices needs to be evaluated for forecasting performance improvement.

*Received 23 May 2021*

## REFERENCES

[1] Lu, C. J. and Wu, J. Y. (2011). An efficient CMAC neural network for stock index forecasting. *Expert Systems with Applications* **38** (12) 15194–15201.

[2] Fadlalla, A. and Amani, F. (2014). Predicting next trading day closing price of qatar exchange index using technical indicators and artificial neural networks. *Intelligent Systems in Accounting, Finance and Management* **21** (4) 209–223.

[3] Hinich, M. J. and Patterson, D. M. (1985). Evidence of nonlinearity in daily stock returns. *Journal of Business & Economic Statistics* **3** (1) 69–77.

[4] Narayan, P. K. (2005). Are the Australian and New Zealand stock prices nonlinear with a unit root? *Applied Economics* **37** (18) 2161–2166.

[5] Lu, C. J. (2010). Integrating independent component analysis-based denoising scheme with neural network for stock price prediction. *Expert Systems with Applications* **37** (10) 7056–7064.

[6] Hassani, H., Soofi, A. S. and Zhigljavsky, A. (2013). Predicting inflation dynamics with singular spectrum analysis. *Journal of the Royal Statistical Society: Series A* **176** (3) 743–760. MR3067422

[7] Coussin, M. (2021). Singular spectrum analysis for real-time financial cycles measurement. *Journal of International Money and Finance* 102532.

[8] Hassani, H., Rua, A., Silva, E. S. and Thomakos, D. (2019). Monthly forecasting of GDP with mixed-frequency multivariate singular spectrum analysis. *International Journal of Forecasting* **35** (4) 1263–1272.

[9] Hassani, H., Yeganegi, M. R. and Gupta, R. (2021). Historical forecasting of interest rate mean and volatility of the united states: Is there a role of uncertainty? *Annals of Financial Economics* **15** (4) 2050018.

[10] Škare, M. and Porada-Rochoń, M. (2020). Multi-channel singular-spectrum analysis of financial cycles in ten developed

economies for 1970–2018. *Journal of Business Research* **112** 567–575.

[11] Patel, J., Shah, S., Thakkar, P. and Kotecha, K. (2015). Predicting stock and stock price index movement using trend deterministic data preparation and machine learning techniques. *Expert Systems with Applications* **42** (1) 259–268.

[12] de Oliveira, F. A., Nobre, C. N. and Zarate, L. E. (2013). Applying artificial neural networks to prediction of stock price and improvement of the directional prediction index–case study of PETR4, Petrobras, Brazil. *Expert Systems with Applications* **40** (18) 7596–7606.

[13] Ticknor, J. L. (2013). A Bayesian regularized artificial neural network for stock market forecasting. *Expert Systems with Applications* **40** (14) 5501–5506.

[14] Kao, L. J., Chiu, C. C., Lu, C. J. and Chang, C. H. (2013). A hybrid approach by integrating wavelet-based feature extraction with MARS and SVR for stock index forecasting. *Decision Support Systems* **54** (3) 1228–1244.

[15] Pai, P. F. and Lin, C. S. (2005). A hybrid ARIMA and support vector machines model in stock price forecasting. *Omega* **33** (6) 497–505.

[16] Wang, J. J., Wang, J. Z., Zhang, Z. G. and Guo, S. P. (2012). Stock index forecasting based on a hybrid model. *Omega* **40** (6) 758–766. MR4269044

[17] Xiao, J., Zhu, X., Huang, C., Yang, X., Wen, F. and Zhong, M. (2019). A new approach for stock price analysis and prediction based on SSA and SVM. *International Journal of Information Technology & Decision Making* **18** (01) 287–310.

[18] Hagfors, L. I., Bunn, D., Kristoffersen, E., Staver, T. T. and Westgaard, S. (2016). Modeling the UK electricity price distributions using quantile regression. *Energy* **102** 231–243.

[19] Nowotarski, J. and Weron, R. (2015). Computing electricity spot price prediction intervals using quantile regression and forecast averaging. *Computational Statistics* **30** (3) 791–803. MR3404360

[20] Khan, M. A. R. and Poskitt, D. S. (2017). Forecasting stochastic processes using singular spectrum analysis: Aspects of the theory and application. *International Journal of Forecasting* **33** (1) 199–213.

[21] Golyandina, N., Nekrutkin, V. and Zhigljavski, A. (2001). *Analysis of time series structure: SSA and related techniques*, CRC Press. MR1823012

[22] Mahmoudvand, R. and Rodrigues, P. C. (2018). A new parsimonious recurrent forecasting model in singular spectrum analysis. *Journal of Forecasting* **37** (2) 191–200. MR3771548

[23] Khan, M. A. R. and Poskitt, D. S. (2013). A note on window length selection in singular spectrum analysis. *Australian & New Zealand Journal of Statistics* **55** (2) 87–108. MR3079022

[24] Chu, M. T. and Lin, M. M. and Wang, L. (2013). A study of singular spectrum analysis with global optimization techniques. *Journal of Global Optimization* **60** (3) 551–574. MR3265245

[25] Harris, T. and Yuan, H. (2010). Filtering and frequency interpretations of singular spectrum analysis. *Physica D: Nonlinear Phenomena* **239** (20) 1958–1967. MR2684605

[26] Khan, A. R. and Hassani, H. (2019). Dependence measures for model selection in singular spectrum analysis. *Journal of the Franklin Institute* **356** (15) 8906–8928. MR4010165

[27] Fuller, W. A. (1996) *Introduction to statistical time series*, John Wiley & Sons. MR1365746

[28] Jarque, C. M. and Bera, A. K. (1980). Efficient tests for normality, homoscedasticity and serial independence of regression residuals. *Economics Letters* **6** (3) 255–259. MR0615323

[29] Cromwell, J. B., Labys, W. C. and Terraza, M. (1994). *Univariate tests for time series models*, Sage University Paper Series on Quantitative Applications in the Social Sciences, 07-099, Sage, Thousand Oaks.

[30] Kwiatkowski, D., Phillips, P. C. , Schmidt, P. and Shin, Y. (1992). Testing the null hypothesis of stationarity against the alternative of a unit root: How sure are we that economic time series have a unit root? *Journal of Econometrics* **54** (1-3) 159–178.

[31] Teräsvirta, T., Lin, C. F. and Granger, C. W. (1993). Power of the neural network linearity test. *Journal of Time Series Analysis* **14** (2) 209–220.

[32] Khan, A. R. and Poskitt, D. S. (2016). Signal identification in singular spectrum analysis. *Australian & New Zealand Journal of Statistics* **58** (1) 71–98. MR3499151

Atikur R. Khan
North South University
Bangladesh
E-mail address: atikur.khan@northsouth.edu

Hossein Hassani
Research Institute of Energy Management and Planning
University of Tehran
Iran
E-mail address: hassani.stat@gmail.com